

RESEARCH

Open Access



# Two novel polyvalent phages: a promising approach for cross-order pathogen control in aquaculture

Chengcheng Li<sup>1,2,3†</sup>, Yufei Yue<sup>1,2,3†</sup>, Rui Yin<sup>1,2,5</sup>, Jiulong Zhao<sup>1,2,3</sup>, Zengmeng Wang<sup>1,2,3</sup>, Shailesh Nair<sup>1,2,3</sup> and Yongyu Zhang<sup>1,2,3,4\*</sup>

## Abstract

Bacteriophages represent a promising alternative to antibiotics for controlling bacterial pathogens. However, phage application is often hindered by its narrow host range in preventing diseases caused by multiple unknown pathogens. While broad-host-range phages capable of cross-genus or cross-order infections, offer significant advantages in addressing this challenge, they are rarely isolated. In this study, we isolated two polyvalent lytic phages, SA-P and SA-M, through a multi-host enrichment strategy. These phages exhibited remarkable cross-order infectivity against the co-occurring aquaculture pathogens *Shewanella algae* and multiple *Vibrio* species. We confirmed that SA-P executes a complete lytic cycle in these cross-order hosts, indicating exceptional compatibility of its lysis systems across taxonomic orders. Genomic analysis revealed that their broad host recognition ability may stem from their diverse tail fiber and tailspike proteins. Notably, SA-P and SA-M are the first phages reported to infect *S. algae*, and their combined application exhibited a sustained suppression of pathogen growth. Proteomic phylogenetic analysis suggests these phages represent a novel unclassified viral genus and family, respectively. This study provides two promising polyvalent phages and their cocktails as potential solution for cross-order pathogen control in aquaculture.

**Keywords** Bacteriophage therapy, Polyvalent phage, Cross-order infection, Pathogen control

## Background

Bacteriophage therapy has emerged as a promising alternative for controlling bacterial pathogens, particularly in the context of increasing antibiotic resistance that threatens environmental safety and human health [1, 2]. Although using phages to prevent or remove pathogens in food animal production, agriculture, and clinical settings has shown positive effects [3–5], the practical application of phage therapy faces several fundamental challenges.

A significant obstacle is the narrow host range exhibited by most phages, which requires the development of diverse phage mixtures or cocktails to effectively combat complex bacterial infections [6–8]. This is currently

<sup>†</sup>Chengcheng Li and Yufei Yue contributed equally to this work.

\*Correspondence:

Yongyu Zhang  
zhangyy@qibebt.ac.cn

<sup>1</sup>Qingdao New Energy Shandong Laboratory, Key Laboratory of Biofuels, Shandong Provincial Key Laboratory of Energy Genetics, Qingdao Institute of Bioenergy and Bioprocess Technology, Chinese Academy of Sciences, Qingdao 266101, China

<sup>2</sup>University of Chinese Academy of Sciences, Beijing 100049, China

<sup>3</sup>Shandong Energy Institute, Qingdao 266101, China

<sup>4</sup>Laboratory for Marine Biology and Biotechnology, Qingdao Marine Science and Technology Center, Qingdao 266237, China

<sup>5</sup>Ocean University of China, Qingdao 266101, China



a major obstacle limiting the widespread application of phages in disease prevention. To address this limitation, researchers have explored several strategies to expand phage host ranges, such as long-term phage-host coevolution and genetic engineering approaches that modify receptor-binding proteins [9, 10]. In environments with taxonomically diverse pathogens, polyvalent phages—capable of targeting multiple bacterial species—exhibit pathogen-suppressive properties comparable to broad-spectrum antibiotics, making them highly promising for therapeutic use [11]. Furthermore, polyvalent phages are much more ubiquitous in natural ecosystems than previously thought based on the metagenomic analyses on environmental samples [12–17]. Notable evidence includes the identification of cross-genus viruses infecting members of the *Sulfolobaceae* family in hot springs [12], as well as putative cross-phylum-infecting viruses detected in sediment samples [17]. However, despite their potential, broad-host range phages (or polyvalent phages) capable of infecting bacteria across divergent genera or even disparate taxonomic orders are rarely isolated [18–21].

In aquaculture, opportunistic pathogens from different taxonomic orders, including *Aeromonas* spp., *Pseudoalteromonas* spp., *Vibrio* spp., and *Shewanella* spp., commonly co-occur and pose significant threats to aquatic species [22, 23]. Amongst them, *Shewanella algae* is a particularly critical marine pathogen of significant epidemiological importance, demonstrating notable pathogenicity across diverse aquatic species [24, 25] and posing substantial risks to human health through contaminated seafood [26]. Concurrently, vibriosis, caused by *Vibrio* spp., remains a predominant disease undermining global aquaculture productivity [27, 28]. In this study, we successfully isolated two cross-order infectivity bacteriophages, SA-P and SA-M, employing a multi-host enrichment approach where hosts from distinctly different taxonomic orders (specifically *S. algae* and nine *Vibrio* strains) served as the bait for phage isolation [29]. Notably, this study presents the first comprehensive report of lytic bacteriophages infecting *S. algae* and provides important insights into the application of polyvalent phages for controlling diverse unknown potential pathogens in aquaculture environments.

## Results

### Cross-order infectivity phages SA-P and SA-M were isolated via a multi-host enrichment phage isolation strategy

A novel bacteriophage, SA-P, was isolated using a multi-host enrichment strategy from a mixed culture containing multiple nine *Vibrio* species and wild-type strain *S. algae* 37 (Table S1). Concurrently, phage SA-M was isolated from a mixture of *Vibrio* species and *S. algae* 37-R,

a strain resistant to SA-P infection (Table S1). Transmission electron microscopy (TEM) analysis revealed two morphologically distinct bacteriophages. SA-P exhibited an icosahedral head of  $51 \pm 2$  nm in diameter with a non-contractile tail of  $331 \pm 7$  nm in length (Fig. 1A). In contrast, SA-M possessed a larger icosahedral head ( $67 \pm 3$  nm in diameter) and a distinct contractile tail ( $147 \pm 5$  nm in length) (Fig. 1B).

The infection patterns of SA-P and SA-M varied across different bacterial hosts. Specifically, phage SA-P demonstrated clear, well-defined lytic zones on the lawns of *S. algae* 37, *Vibrio sagamiensis* XJ001, and *Vibrio parahaemolyticus* 05–1, whereas it produced diffuse and less distinct lysis zones on alternative host strains *Vibrio mytili* XJK003 (Fig. S1). In contrast, phage SA-M exclusively formed distinct lytic zones on *S. algae* 37 and six *S. algae* 37-resistant strains lawns (Fig. S2), while forming cloudy zones on the lawns of *Shewanella upenei* XJK015, *Shewanella upenei* HNX001, *Vibrio mytili* XJK003, and *Vibrio sagamiensis* FB1020 (Fig. S1).

Double-layer plate assays indicated that SA-M could form plaques only on *S. algae* lawns, suggesting host-specific replication (Fig. 1C). In comparison, SA-P demonstrated more versatile replication, effectively propagating on multiple hosts, including *S. algae*, *V. parahaemolyticus*, and *V. sagamiensis* (Fig. 1D). Furthermore, while the OD<sub>600</sub> of the control bacteria reached around 1, the growth of *S. algae*, *V. parahaemolyticus*, and *V. sagamiensis* was suppressed by SA-P to 0.18–0.27, 0.56–0.61, and 0.29–0.43, respectively, within about 7 h at MOIs of 0.1 and 1 (Fig. 2). The ability of SA-P and SA-M to infect multiple bacterial species across different orders underscores their potential as versatile biocontrol agents in aquaculture management.

### Infection characteristic of phages SA-P and SA-M

#### (1) One-step growth curves

*S. algae* was employed as a host to evaluate the infection characteristics of phages SA-P and SA-M. In particular, one-step growth curves revealed distinct life cycle parameters between SA-P and SA-M. During incubation with *S. algae* 37, SA-P demonstrated rapid infection dynamics with a latent period (30 min), efficient virion production (burst size of 116 PFU/cell), and a complete lytic cycle of 75 min (Fig. 3A). In contrast, SA-M demonstrated a shorter latent period (<20 min), a burst size of 13 PFU/cell, and a complete lytic cycle of 80 min (Fig. 3B). Notably, while the *S. algae* 37-R strain was resistant to SA-P, SA-M demonstrated lytic activity against this variant, with a prolonged latent period of 90 min and a burst size of 35 PFU/cell (Fig. 3C).

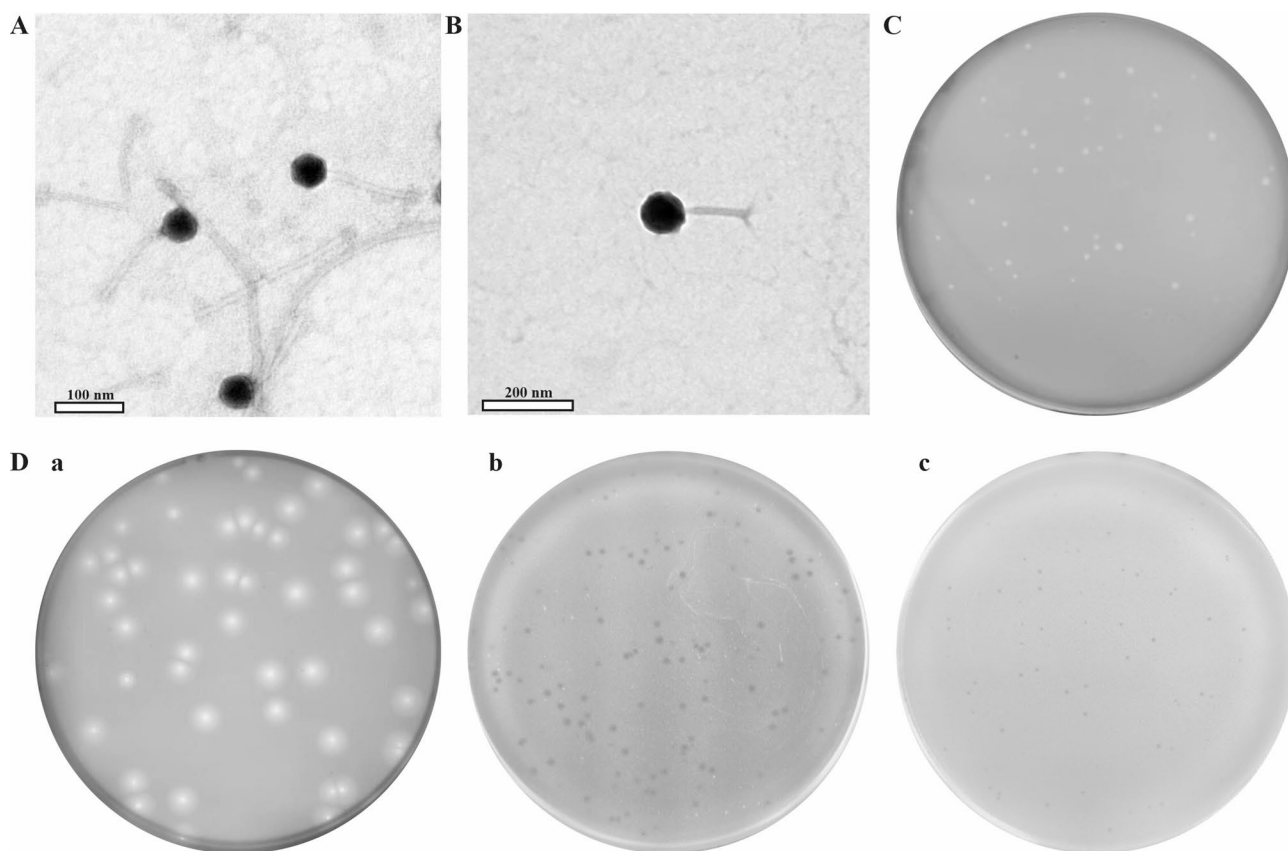


**Fig. 1** Transmission electron microscopy characterization of bacteriophages SA-P (A) and SA-M (B). Representative phage plaque morphologies on double-layer agar plates illustrating the replication efficacy of SA-M in *S. algae* (C) and SA-P across diverse pathogenic strains (D), specifically *S. algae* (a), *V. sagamiensis* (b), and *V. parahaemolyticus* (c)

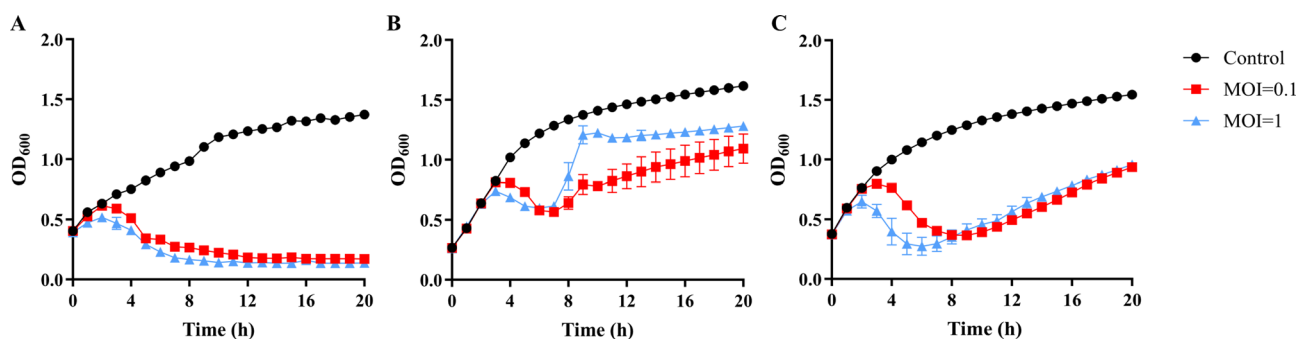


**Fig. 2** The growth curves of *S. algae* 37 (A), *V. parahaemolyticus* (B), and *V. sagamiensis* (C) upon infection by bacteriophage SA-P at MOIs of 0.1 and 1

## (2) environmental stability

Both phages maintained lytic efficiency across a broad pH range (5–9), with optimal infectivity observed between pH 7–8 (Fig. 3D). Temperature sensitivity assays revealed that both phages maintained high stability between 4 °C and 30 °C, followed by a progressive decline in viability between 40 °C and 50 °C, with complete inactivation occurring above 60 °C (Fig. 3E). This pH and temperature tolerance suggests that these phages could maintain their infective capabilities when applied for pathogen control in aquaculture settings [30]. Additionally, both phages

demonstrated chloroform resistance, indicating the absence of lipid components in their capsids (Fig. S3).

## (3) A combination of phages SA-P and SA-M demonstrated sustained inhibition of *S. algae* in comparison to single-phage treatment

The growth curve of host bacteria *S. algae* treated with either single-phage (SA-P or SA-M) and combination (SA-P and SA-M) were investigated. Individual phage infections initially induced rapid bacterial decline within 10–24 h post-infection (Fig. 3F). However, bacterial

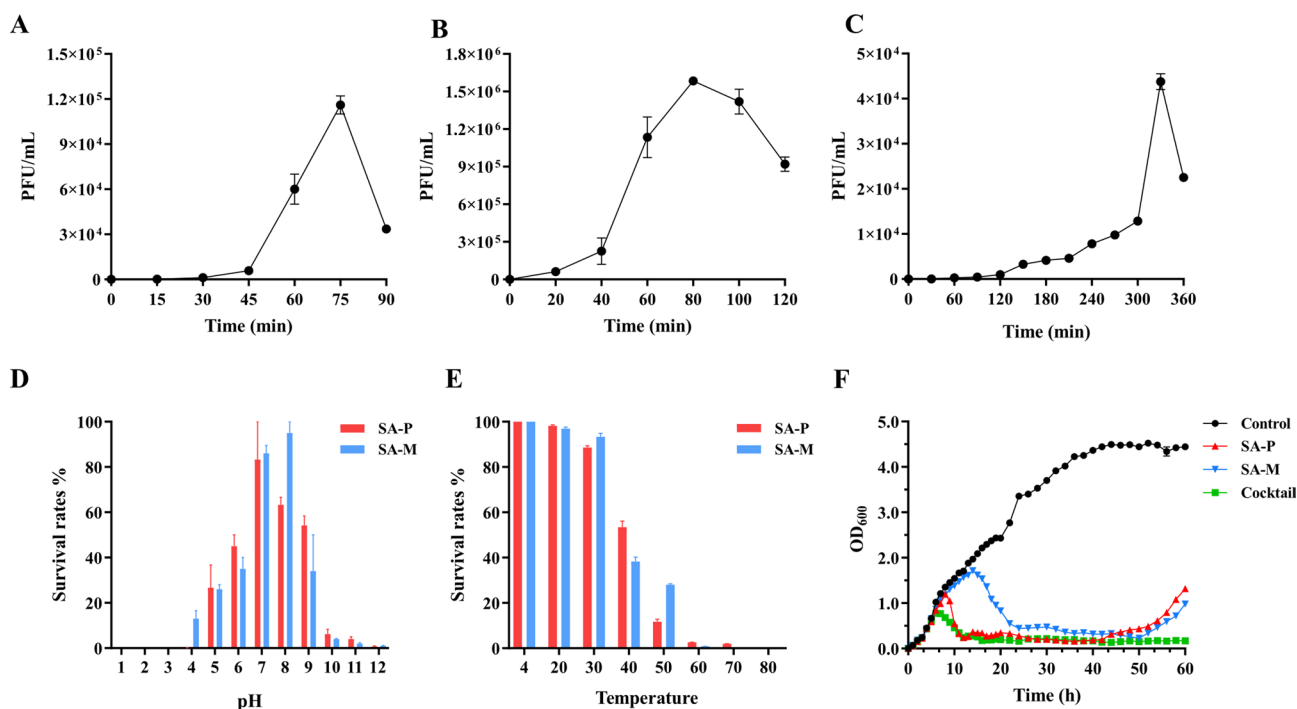


**Fig. 3** Comprehensive bacteriophage characterization. One-step growth curve of SA-P (A) and SA-M (B) infecting wild-type *S. algae* 37; (C) One-step growth curve of SA-M infecting *S. algae* 37-R; The sensitivity of both phages to pH (D) and Temperature (E); The growth curves of *S. algae* 37 infected by phage SA-P, and SA-M and their combinations at a MOI of 0.1 (F)

regrowth was observed after 50 h ( $OD_{600}$  reaching 1.5–1.8 at 60 h), likely due to the emergence of phage-resistant variants. In contrast, a combination of SA-P/SA-M maintained a significant suppression of bacterial growth ( $OD_{600} < 0.4$ ,  $p$ -value  $< 0.05$ ) throughout the 60-h experimental period. Furthermore, a combination of phages SA-P/SA-M demonstrated an expanded host range (8 strains) compared to either single phage alone (4 strains for SA-P, 6 strains for SA-M) (Table 1). This sustained inhibition and broader host range suggested that an SA-P/SA-M phage cocktail offers promising potential for *S. algae* control while effectively circumventing the development of bacterial phage resistance [31].

#### Genomic characterization and phylogenetic analysis of SA-P and SA-M

Comparative genomic analysis revealed striking differences in genome organization and content between the two phages (Table 2). SA-P possessed a relatively compact circular double-stranded DNA genome (73,444 bp, GC content of 44.05%), encoding 100 open reading frames (ORFs), of which 43 demonstrated significant homology to characterized functions. In contrast, SA-M contained a substantially larger linear double-stranded DNA genome (276,582 bp, GC content of 36.16%), with 368 ORFs, including 138 functionally annotated ORFs. The DNA packaging strategy was predicted to be unknown for both SA-P and SA-M. Both genomes

encoded essential viral proteins, including DNA replication (helicase), DNA metabolism (exonuclease), DNA packaging (terminase large/small subunit), and structural components (capsid proteins) (Fig. 4A and B). Both SA-P and SA-M genomes contain the *recA* gene, which known to facilitate prophage excision, cell lysis, and potential lytic-to-lysogenic state transitions [32, 33]. However, no integrase genes were detected in either genome, and no lysogenic activity was observed under our experimental conditions (Fig. S4). Importantly, genomic analysis revealed no genes associated with antibiotic resistance, toxins, or pathogenicity factors, supporting the safety profile of these phages for aquaculture applications [34].

BLASTn analysis against the NCBI database identified *Vibrio* phage vB\_VhaP\_PG11 as the closest relative to phage SA-P (78.54% sequence identity, 4% query coverage). Remarkably, no significant matches were found for the SA-M genome, highlighting the novelty of these phages [35]. Phylogenetic analysis based on whole-proteome comparison (Fig. 4C) positioned SA-P within *Schistoviridae*, suggesting its classification as a novel genus within this family. SA-M formed a distinct phylogenetic branch separate from other phages, indicating that it likely represents a novel family within *Caudoviricetes*.



**Table 1** Host range of phages SA-P, SA-M, and the combination

Species	Strain	SA-P	SA-M	Combination
<i>Shewanella algae</i>	37*	+	+	+
<i>Shewanella algae</i>	37-R*	-	+	+
<i>Shewanella upenei</i>	XJK015*	-	+	+
<i>Shewanella upenei</i>	HNX001	-	+	+
<i>Shewanella indica</i>	KJW27	-	-	-
<i>Shewanella chilikensis</i>	XFB1005*	-	-	-
<i>Vibrio alginolyticus</i>	283*	-	-	-
<i>Vibrio alginolyticus</i>	TFB2020	-	-	-
<i>Vibrio alginolyticus</i>	HS05-8	-	-	-
<i>Vibrio alginolyticus</i>	G1	-	-	-
<i>Vibrio baumannii</i>	HS2-2	-	-	-
<i>Vibrio bivalvicida</i>	HS3-1	-	-	-
<i>Vibrio campbellii</i>	18-1*	-	-	-
<i>Vibrio campbellii</i>	25,005	-	-	-
<i>Vibrio fortis</i>	HS3-4	-	-	-
<i>Vibrio harveyi</i>	VIB645*	-	-	-
<i>Vibrio harveyi</i>	17X-5-1	-	-	-
<i>Vibrio helialis</i>	25,001	-	-	-
<i>Vibrio helialis</i>	17 S-2-3	-	-	-
<i>Vibrio helialis</i>	HNXS003	-	-	-
<i>Vibrio hepatica</i>	HS4-3	-	-	-
<i>Vibrio hepatica</i>	HS4-3	-	-	-
<i>Vibrio hyugaensis</i>	HNXS003*	-	-	-
<i>Vibrio kanaro</i>	HS4-4	-	-	-
<i>Vibrio maximus</i>	pmp022	-	-	-
<i>Vibrio maximus</i>	pmp022-T	-	-	-
<i>Vibrio mytili</i>	XJK003*	+	+	+
<i>Vibrio natriegens</i>	15*	-	-	-
<i>Vibrio neocaledonicus</i>	B19	-	-	-
<i>Vibrio parahaemolyticus</i>	05-1	+	-	+
<i>Vibrio parahaemolyticus</i>	Vp*	-	-	-
<i>Vibrio parahaemolyticus</i>	pmp116	-	-	-
<i>Vibrio reinhardtii</i>	T-HJ001	-	-	-
<i>Vibrio rotiferianus</i>	25,006	-	-	-
<i>Vibrio sagamiensis</i>	FB1020*	-	+	+
<i>Vibrio sagamiensis</i>	XJ001	+	-	+
<i>Vibrio sagamiensis</i>	HNX004	-	-	-
<i>Vibrio sinaloensis</i>	ZZ006*	-	-	-
<i>Vibrio sinaloensis</i>	25,004	-	-	-
<i>Vibrio sinaloensis</i>	ZZ006-T	-	-	-
<i>Vibrio vulnificus</i>	JK018	-	-	-
<i>Vibrio jasicida</i>	B2	-	-	-
<i>Vibrio Atlantic</i>	E-HMS2016	-	-	-

+, Lysed; -, not lysed. \* Pathogens used in simultaneous enrichment during the multi-host phage-isolation strategy

**Table 2** Basic genome characteristics of phages SA-P and SA-M

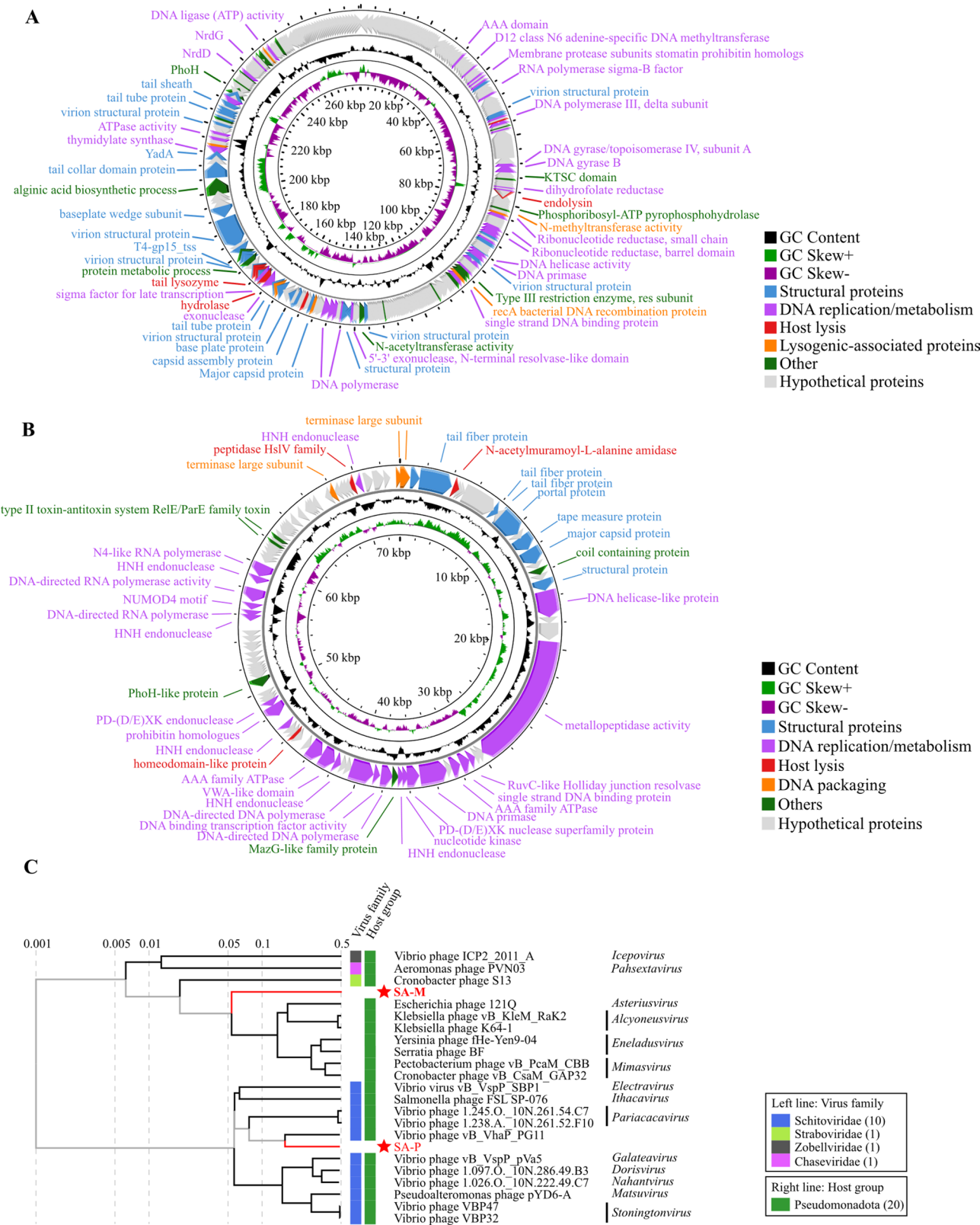
Characteristic	SA-P	SA-M
Genome length (bp)	73,444	276,582
No. of GC content (%)	44.05	36.16
tRNA	2	28
ORFs	100	368
Functionally annotated ORFs	43	138

## Discussion

Phylogenetically distinct bacterial lineages frequently coexist in diverse environmental niches, including water, soil, and animal-associated microbiomes [36–38]. In aquaculture, opportunistic pathogens from different orders, including *Aeromonas* spp., *Pseudoalteromonas* spp., *Vibrio* spp., and *Shewanella* spp., frequently emerge as co-occurring disease agents affecting diverse aquatic species [22, 23]. Broad host range phages, characterized by cross-genus or cross-order infectivity, demonstrate remarkable therapeutic potential analogous to broad-spectrum antibiotics in these environments harboring taxonomically diverse pathogenic populations [11]. However, most isolated phages exhibit intra-genus infectivity, and polyvalent phages with cross-order infectivity were rarely isolated despite their anticipated prevalence in natural environments [12, 18–21].

In this study, we successfully isolated two phages SA-P and SA-M through a multi-host enrichment strategy involving an enriched host mixture containing pathogens from disparate taxonomic orders, which demonstrated cross-order infectivity against *S. algae* and *Vibrio* species. The mixed hosts may exert multiple selective pressures on environmental phages [39] and influences phage evolution through reciprocal selection pressures during phage-host interactions [40–43], potentially increasing the likelihood of isolating polyvalent phages with enhanced isolation efficiency [29].

The broad host range of phages likely results from multiple molecular interactions throughout the infection cycle [7], including diverse receptor-binding proteins (RBPs) [19, 44], mutations in hypervariable domains of RBP-encoding genes [45–47], adaptation to host molecular mechanisms (e.g., codon usage) [48–50], and evasion of intracellular defense systems [50]. Key structural features that potentially enable the broad host range of SA-P and SA-M were analyzed through genomic characterization. Notably, SA-P and SA-M encode three and six different tail fiber/tailspike proteins, respectively, potentially facilitating attachment to diverse bacterial host receptors across genera [19]. The baseplate structures of both phages appear to employ a “Swiss army knife-like” configuration, with multiple tail fibers and tailspikes facilitating adaptable host recognition mechanisms and conferring polyvalent capabilities [51]. Broad-host-range phages typically employ compatible lysis systems, specifically the holin-endolysin system, for efficient progeny release from diverse host cells. Within this system, holins generate lesions in the cytoplasmic membrane, enabling endolysins to access and degrade the murein layer, ultimately leading to cell lysis and phage release [52]. The plaque assays demonstrated that phage SA-P successfully released progeny in both *S. algae* and *Vibrio* species, indicating the compatibility of its holin-endolysin system



with these phylogenetically distinct bacteria. Nevertheless, given the substantial percentage of unannotated genes in the genomes of SA-P (57%) and SA-M (62.5%), further research is needed to fully elucidate their broad host range mechanisms.

Importantly, SA-M demonstrated the ability to infect SA-P-resistant bacteria, revealing distinct host ranges and divergent infection mechanisms between these two phages. This complementarity aligns with the emerging promise of phage cocktails, which have gained attention as an approach to achieve a broad host range and combat bacterial resistance [53, 54]. The unique characteristics of SA-M, which belongs to the giant phage group (genome sizes 200–500 kb) [55], make it particularly valuable in such cocktails. SA-M's expanded repertoire of 28 tRNAs (compared to SA-P's 2 tRNAs) may serve multiple functions: substituting for cleaved host tRNAs during bacterial defense responses, facilitating efficient translation of phage-specific genes through codon optimization [56, 57], and conferring greater independence from host molecular machinery [58]. Furthermore, SA-M harbors four potential stress defense genes—phosphate starvation protein PhoH (ORF 298) [35], Clp protease (ORF 325) [59], glutaredoxin-family protein (ORF 309) [60], and periplasmic protein (ORF 322) [61]—compared to SA-P's single stress defense gene (ORF 52). These genes collectively enhance viral resilience under stressful environmental conditions [62]. Although not yet verified, the potential formation of a phage nucleus by SA-M, characteristic of jumbo phages, may provide additional protection against DNA-targeting CRISPR-Cas systems and restriction enzymes [55, 63], further supporting its value in phage cocktails through complementing SA-P's host range and enhancing overall therapeutic efficacy.

Both phages encode domains that may play a role in bacterial immunity against other bacteriophages [64–66]. SA-M contains an HD domain protein (ORF 64) associated with CRISPR-Cas systems, exhibiting both endo- and exonucleolytic (3'–5') activity against ssDNA and RNA [67]. SA-P harbors a MazG domain (ORF 31), potentially regulating bacterial growth by reducing intracellular guanosine 3',5'-bispyrophosphate (ppGpp) levels [68]. Both phages also contain VWA-like domains, commonly found in phage defense systems [69]. The presence of these regulatory and defensive domains underscores the importance of evaluating their interactions and potential compatibility when deployed alongside other phages in therapeutic cocktails [70].

In addition to whole-phage therapies, there is growing interest in exploiting phage-encoded lytic and bacteriostatic proteins as next-generation antibacterial agents [71, 72]. SA-M encodes endolysin (ORF 113), transglycosylase (ORF 87) and lysozymes (ORFs 255, 256), while SA-P encodes pectate lyase (ORF 3),

N-acetylmuramoyl-L-alanine amidase (ORF 4), and metallopeptidase (ORF 21). These proteins may possess therapeutic antibacterial properties [71–73]. Additional regulatory elements include a phage-encoded N-acetyltransferase (ORF 220) in SA-M, potentially involved in bacterial transcriptional inactivation [74].

Interestingly, our study demonstrated that the SA-P phage exhibited a stronger inhibitory effect against *Vibrio parahaemolyticus* at a low multiplicity of infection (MOI) of 0.1 compared to a higher MOI of 1.0. While elevated MOIs are typically assumed to enhance bactericidal activity by increasing the probability of host infection, our findings align with previous studies indicating that high MOIs can paradoxically diminish phage efficacy. One explanation is the phenomenon of lysis from without, wherein an overwhelming phage-to-host ratio triggers premature bacterial lysis without productive infection, thereby curtailing phage progeny release and disrupting subsequent infection cycles [75]. Furthermore, high MOIs may rapidly deplete susceptible host populations, limiting opportunities for phage amplification and sustained bacterial suppression [76, 77]. Additionally, elevated phage concentrations may activate bacterial defense mechanisms. For instance, increased MOI has been shown to accelerate spacer acquisition in the CRISPR arrays of *Sulfolobus islandicus* LAL14/1, bolstering adaptive immunity against phage predation [78]. Thus, excessive phage densities may activate stress-induced or density-dependent defenses, impairing productive phage replication. In contrast, lower MOIs are less likely to trigger such responses, thereby facilitating more efficient phage propagation and prolonged antibacterial activity. Similar outcomes have been documented in other phage-bacteria systems, where reduced MOIs yielded superior bacterial suppression compared to higher MOIs [79, 80]. Collectively, these findings highlight the critical role of MOI optimization in phage-based applications, as higher phage doses do not invariably correlate with improved clearance and may even compromise efficacy.

## Conclusions

This study represents a significant advancement in aquaculture health management through successfully isolating phages with cross-order infectivity, capable of lysing pathogenic *Shewanella algae* and *Vibrio* species. Future investigations should focus on elucidating the molecular mechanisms underlying the phages' broad host range and optimizing their applications for effective pathogen control in aquaculture.

## Methods and materials

### Phage isolation and purification

*S. algae* 37, isolated from diseased shrimp tissues, was used as the host for phage SA-P isolation. The host strain was cultured in 2216E medium (Hope Bio-Technology, Qingdao, China) at 28 °C with shaking. Water samples collected from the coast of the Yellow Sea, China, were filtered through 0.22-μm sterile microfilters and co-cultured with multiple log-phase host cultures, including *S. algae* 37, *Shewanella chilikensis*, *Shewanella upenei*, and 9 *Vibrio* species. Phage samples were collected and filter-sterilized daily for five consecutive days. Plaque assays were performed by the double-layer agar plating method to determine phage infection [81]. Briefly, 1 mL of the filtrate was serially diluted with SM buffer, and inoculated with 1 mL of log-phase *S. algae* 37 for 30 min at 28 °C in a shaker. The suspension was then mixed with 5 mL of sterile soft 2216E agar (0.5%) and overlaid onto 2216E agar plate (1.5%). Following overnight incubation at 30 °C, a single phage plaque was isolated, resuspended in 1 mL SM buffer (100 mM NaCl, 8 mM MgSO<sub>4</sub>, 50 mM Tris-HCl [pH=7.5]), and purified five times following the double-layer agar plating method described above.

A SA-P-resistant strain, designated *S. algae* 37-R, was subsequently employed as the host for the isolation of novel phage SA-M, from Yellow Sea coastal waters following the aforementioned procedure. To establish methodological controls, additional bacteriophages were isolated through co-cultivation with individual bacterial strains (*Vibrio* spp. and *Shewanella* spp.). All bacterial strains and purified phages were preserved long-term in 0.85% NaCl solution containing 15% glycerol at -80 °C.

### Host range testing

The host range of these phages was determined using spot tests [82] against a panel of 53 bacterial strains from our laboratory collection, including 10 SA-P-resistant *Shewanella* isolates. In brief, 1 mL of a log-phase bacterial aliquot was mixed with 4 mL molten 2216E (0.5% agar) and overlaid onto 2216E agar plate (1.5% agar). Ten-microliter aliquots of phage suspension (10 μL) were spotted onto these double-layer agar plates and incubated overnight at 28 °C. The bacterial sensitivity to phages was determined by the presence of clear lysis zones at the spot. Furthermore, to evaluate the replicative capacity of bacteriophages in specific bacterial hosts, serial-diluted phage lysates and host cultures were mixed with molten 2216E medium and subsequently spread onto solid 2216E agar plates. After incubating at 28 °C for 24 h, the phages' host-specific replication was determined by the presence of plaques [83].

### Antimicrobial activity assessment of SA-P against diverse hosts

The antimicrobial activity of phage SA-P was evaluated against three bacterial strains: *Shewanella algae* 37, *Vibrio sagamiensis* XJ001, and *Vibrio parahaemolyticus* 05-1. Briefly, bacterial cultures (800-μL aliquots, initial concentration  $1 \times 10^8$  CFU/mL) were inoculated into 48-well microtiter plates (Nest Biotechnology, China) and infected with SA-P at multiplicities of infection (MOI) of 0.1 and 1.0. Control wells without phage were included to monitor bacterial growth in the absence of phage treatment. Cultures were incubated at 28 °C with shaking at 150 rpm, and bacterial growth was monitored by measuring optical density at 600 nm (OD<sub>600</sub>) at 1-hour intervals using a microplate reader (TECAN, Infinite 200 PRO, Switzerland). All assays were conducted in triplicate to ensure reproducibility. This approach enabled a comparative assessment of SA-P's inhibitory effect against different host strains under controlled conditions.

### Antimicrobial activity assessment of individual phages and cocktails against *S. algae*

The antimicrobial efficacy of phages SA-P, SA-M, and their combination was tested against *S. algae* 37. Bacteria cultures were inoculated at 1% (v/v) into fresh medium (100 mL) and incubated at 28 °C with shaking conditions (150 rpm) until reaching log-phase (OD<sub>600</sub> = 0.6). Phages were then added at MOI=0.1, while control groups received an equal volume of 2216E medium. OD<sub>600</sub> measurements were taken at 1-hour intervals for the first 20 h, followed by measurements at 2-hour intervals, using a UV spectrophotometer (WPA Biowave II, Biochrom, England). All assays were performed in triplicate.

### Phage morphology characterization

Phage morphology was characterized using Transmission Electron Microscopy (TEM) [84]. Briefly, the phage lysates were concentrated using a 30-kDa ultrafiltration membrane and washed three times with SM buffer. A 10-μL aliquot of concentrated phage suspension was deposited on a 200-mesh carbon-coated copper grid and air-dried. Phage particles were then negatively stained with 2% uranyl acetate for 3 min. TEM observations were performed at magnifications between 20,000 × and 30,000 × using a Hitachi-7800 instrument operating at 80 kV.

### One-step growth curve

Phage life cycles were determined using a modified one-step growth curve method [85]. In brief, 1 mL of log-phase bacteria culture (OD<sub>600</sub>=0.6) was mixed with a phage suspension at a multiplicity of infection (MOI) of 0.01. After 20 min of adsorption, the mixture was centrifuged (5000 × g, 3 min), and the pellet was washed three



times with 2216E medium to remove unadsorbed phages. Subsequently, the pellets were resuspended in 1 mL 2216E medium, and 20- $\mu$ L resuspension was transferred to 20 mL fresh medium incubating at 28 °C with shaking, making the initial infection timepoint ( $T_0$ ). Phage titers were measured at 15 to 30-minute intervals using double-layer agar plaque assays. The burst size was calculated as:  $\text{Burst size} = (\text{PFU}_{\text{final}} - \text{PFU}_{T_0}) / (\text{PFU}_{\text{added}} - \text{PFU}_{T_0})$ .

### Phage stability analysis

For pH stability testing, phage lysates were inoculated in SM buffer with pH values ranging from 1 to 12 at 28 °C for 1 h [30]. Following pH neutralization, phage titers and survival rates were determined using the double-layer agar method. In the thermostability assessment, phage lysates (108 PFU/mL) were subjected to temperature-controlled incubation at 20, 30, 40, 50, 60, 70, and 80 °C for 1 h, after which phage titers were quantified using the standard double-layer agar methodology. Chloroform sensitivity was assessed by mixing 1 mL of phage lysate with 20 mL (i.e., 2% [vol/vol]) and 200 mL (i.e., 20% [vol/vol]) of pure chloroform [84]. Mixtures were vigorously agitated for 1 min, incubated at room temperature for 30 min, then centrifuged at  $6,000 \times g$  for 5 min. The phage-containing supernatants were spotted on *S. algae* 37 lawn to assess phage activity.

### Lysogeny test

For the lysogeny investigation of phages SA-M and SA-P, a modified protocol was employed [33]. Briefly, phage-resistant strains were isolated as previously described [86] and PCR analysis was performed to detect potential integrated phage genome fragments within these phage-resistant strains. Wild-type strain served as negative controls and phages served as positive controls. PCR amplification targeted specific phage sequences using the following primers: for SA-P, PF1 (5'-ACTCTTCTGAAG TTGGAACG-3') and PR1 (5'-CAGATCGTGGCATGTA AGAA-3'); for SA-M, MF1 (5'-GATAATTCATTCATGT CAACGTC-3') and MR1 (5'-CAGAAATCTGAAATCGT AA-3').

### Genome DNA extraction, sequencing, and analysis

Phage DNA was extracted using the DNeasy Blood & Tissue Kit (QIAGEN) according to the manufacturer's instructions [87]. High-throughput sequencing was constructed using the Illumina NovaSeq X plus platform (Illumina Inc., San Diego, CA, USA) by Qingdao OE Biotech Co., Ltd. (Qingdao, China). The libraries were constructed with VAHTS Universal Plus DNA Library Prep Kit (Vazyme, Nanjing, China). Raw reads were quality-filtered by the KneadData (v0.10.0) and assembled using SPAdes Genome Assembler (v3.14.1) [88]. Non-viral sequences were removed using CheckV (v0.7.0) [89].

Open reading frames (ORFs) were predicted using GeneMarks [90] and Prokka (v1.14.6) [91], then annotated by BLASTp against the nonredundant (nr) protein database of the NCBI (<https://www.ncbi.nlm.nih.gov/>) with an e-value of  $10^{-5}$ . PhageScope (v1.3) [92] was used for tRNAs, virulence genes, and antimicrobial resistance gene prediction. PhageTerm was used to predict the genome termini and phage packaging mechanisms [93]. Genome visualization was performed using Proksee server [94]. Proteomic tree based on genomic similarity ( $S_G$  score) was generated using ViPTree 4.0 [95].

After genome sequencing, PCR amplifications were carried out to check whether these genomes were circular or linear using the following primers: SA-PF (5'-AG ACTACCTAAATGAGGTGG-3'), SA-PR (5'-GTACACG TCGTTTTGTTGATC-3'), SA-MF (5'-ACAAACCCAGA TGCTTACAC-3'), and SA-MR (5'-AATATGGACCACC GAGAAGAT-3'). These primers were designed to extend outward from the termini of the putative linear genomes. PCR amplification products would be generated only from circular genomes, with sequences consistent with the assembled genome sequence.

### Statistical analysis

All experiments were performed in biological triplicates. Data were analyzed using GraphPad Prism 9 software [96]. One-way analysis of variance (ANOVA) followed by Tukey's multiple comparisons test was used to assess statistical significance between groups. A  $p$ -value  $\leq 0.05$  was considered statistically significant.

### Supplementary Information

The online version contains supplementary material available at <https://doi.org/10.1186/s12985-025-02817-4>.

Supplementary Material 1

### Acknowledgements

This work was supported by the projects of Natural Science Foundation of China (No. 42476115, 42106107, 42406120, 42206124, 42350410437), Taishan Industrial Experts Programme (tscy2024116), the Shandong Province Postdoctoral Fund Project - SDBX2022030, the Postdoctoral Fellowship Program of CPSF (No. GZC20232809), the Qingdao Postdoctoral Fund Project (No. QDBSH20240102185), and the Ocean Negative Carbon Emissions (ONCE) Program.

### Author contributions

CL: experiments, manuscript writing, and data analysis. YY: data analysis and manuscript writing. RY: phage isolation and characterization. JZ, ZW, and SN: data analysis and discussion. YZ: study design, supervision, writing-reviewing and editing.

### Funding

This work was supported by the projects of Natural Science Foundation of China (No. 42476115, 42106107, 42406120, 42206124, 42350410437), Taishan Industrial Experts Programme (tscy2024116), the Shandong Province Postdoctoral Fund Project - SDBX2022030, the Postdoctoral Fellowship Program of CPSF (No. GZC20232809), the Qingdao Postdoctoral Fund Project (No. QDBSH20240102185), and the Ocean Negative Carbon Emissions (ONCE) Program.

### Data availability

The complete genome sequence of phages SA-P and SA-M was deposited at NCBI GenBank under accession numbers PQ510824 and PQ510825, respectively.

### Declarations

#### Ethics approval and consent to participate

Not applicable.

#### Consent for publication

Not applicable.

#### Competing interests

The authors declare no competing interests.

Received: 26 February 2025 / Accepted: 29 May 2025

Published online: 07 June 2025

### References

- Pimenta R. Role of bacteriophages in targeting antibiotic resistant bacteria. *Int J Sci Res (JSR)*. 2023;12:1639–42.
- Sagar S, Kaistha S, Das AJ, Kumar R. Bacteriophage: a new hope for the control of antibiotic-resistant bacteria. In *Antibiotic resistant bacteria: a challenge to modern medicine*. Edited by Sagar S, Kaistha S, Das AJ, Kumar R. Singapore: Springer Singapore. 2019;153–164.
- Goodridge LD. Application of bacteriophages to control pathogens in food animal production. In *Bacteriophages in the control of food- and waterborne pathogens*. 2010; 61–77.
- Jamal M, Bukhari SMAUS, Andleeb S, Ali M, Raza S, Nawaz MA, Hussain T, Rahman Su, Shah SSA. Bacteriophages: an overview of the control strategies against multiple bacterial infections in different fields. *J Basic Microbiol*. 2019;59:123–33.
- Greer GG. Bacteriophage control of foodborne bacteria. *J Food Prot*. 2005;68:1102–11.
- Immadi Siva R. Phage therapy: challenges and opportunities. *Fine Focus*. 2022;8:12–35.
- de Jonge PA, Nobrega FL, Brouns SJJ, Dutilh BE. Molecular and evolutionary determinants of bacteriophage host range. *Trends Microbiol*. 2019;27:51–63.
- Droubogiannis S, Katharios P. Phage therapy in aquaculture. In *Antimicrobial resistance in aquaculture and aquatic environments*. Edited by Elumalai P, Lakshmi S. Singapore: Springer Nature Singapore. 2025;229–255.
- Ando H, Lemire S, Pires Diana P, Lu Timothy K. Engineering modular viral scaffolds for targeted bacterial population editing. *Cell Syst*. 2015;1:187–96.
- Chen M, Zhang L, Abdelgader Sheikheldin A, Yu L, Xu J, Yao H, Lu C, Zhang W. Alterations in gp37 expand the host range of a T4-like phage. *Appl Environ Microbiol*. 2017;83:e01576–01517.
- Chung KM, Liao XL, Tang SS. Bacteriophages and their host range in multidrug-resistant bacterial disease treatment. In *Pharmaceuticals*. 16;2023.
- Munson-McGee JH, Peng S, Dewerff S, Stepanauskas R, Whitaker RJ, Weitz JS, Young MJ. A virus or more in (nearly) every cell: ubiquitous networks of virus–host interactions in extreme environments. *ISME J*. 2018;12:1706–14.
- Paez-Espino D, Elie-Fadrosh EA, Pavlopoulos GA, Thomas AD, Huntemann M, Mikhailova N, Rubin E, Ivanova NN, Kyrpides NC. Uncovering earth's Virome. *Nature*. 2016;536:425–30.
- Wu R, Davison Michelle R, Nelson William C, Graham Emily B, Fansler Sarah J, Farris Y, Bell Sheryl L, Godinez I, McDermott Jason E, Hofmoeck Kirsten S, Jansson Janet K. DNA viral diversity, abundance, and functional potential vary across grassland soils with a range of historical moisture regimes. *mBio*. 2021;12:e02595–02521.
- Trubl G, Kimbrel JA, Lique-Gonzalez J, Nuccio EE, Weber PK, Pett-Ridge J, Jansson JK, Waldrop MP, Blazewicz SJ. Active virus–host interactions at sub-freezing temperatures in Arctic peat soil. *Microbiome*. 2021;9:208.
- Li Z, Pan D, Wei G, Pi W, Zhang C, Wang J-H, Peng Y, Zhang L, Wang Y, Hubert CRJ, Dong X. Deep sea sediments associated with cold seeps are a subsurface reservoir of viral diversity. *ISME J*. 2021;15:2366–78.
- Hwang Y, Roux S, Coclet C, Krause SJE, Girguis PR. Viruses interact with hosts that span distantly related microbial domains in dense hydrothermal Mats. *Nat Microbiol*. 2023;8:946–57.
- Kim S, Kim S-H, Rahman M, Kim J. Characterization of a Salmonella Enteritidis bacteriophage showing broad lytic activity against Gram-negative enteric bacteria. *J Microbiol*. 2018;56:917–25.
- Schwarzer D, Buettner Falk FR, Browning C, Nazarov S, Rabsch W, Bethe A, Oberbeck A, Bowman Valerie D, Stummeyer K, Mühlenhoff M, et al. A multi-valent adsorption apparatus explains the broad host range of phage phi92: a comprehensive genomic and structural analysis. *J Virol*. 2012;86:10384–98.
- Malki K, Kula A, Bruder K, Sible E, Hatzopoulos T, Steidel S, Watkins SC, Putonti C. Bacteriophages isolated from lake Michigan demonstrate broad host-range across several bacterial phyla. *Virol J*. 2015;12:164.
- Bozidis P, Markou E, Gouni A, Gartzonika K. Does phage therapy need a pan-phage? In *pathogens*, vol. 13; 2024.
- Abou-Okada. In: Fisheries, et al. editors. Winter kills in farmed European Seabass (*Dicentrarchus labrax*): co-infected with *Shewanella putrefaciens* and *Aeromonas veronii*. *MJEJoAB*; 2022.
- Li H, Qiao G, Gu J-Q, Zhou W, Li Q, Woo S-H, Xu D-H, Park S-I. Phenotypic and genetic characterization of bacteria isolated from diseased cultured sea cucumber *Apostichopus japonicus* in Northeastern China. *Dis Aquat Organ*. 2010;91:223–35.
- Wang L, Chen S, Xing M, Dong L, Zhu H, Lin Y, Li J, Sun T, Zhu X, Wang X. Genome characterization of *Shewanella* algae in Hainan province, China. *Front Microbiol*. 2024; 15.
- Han Z, Sun J, Lv A, Sung Y, Shi H, Hu X, Xing K. Isolation, identification and characterization of *Shewanella* algae from reared tongue sole, *Cynoglossus semilaevis* Günther. *Aquaculture*. 2017;468:356–62.
- Cao H, Chen S, Lu L, An J. *Shewanella* algae: an emerging pathogen of black spot disease in freshwater-cultured whiteleg shrimp (*Penaeus vannamei*). *J Aquaculture-Bamidgh*. 2018; 70.
- Arunkumar M, LewisOscar F, Thajuddin N, Pugazhendhi A, Nithya C. In vitro and in vivo biofilm forming *Vibrio* spp: A significant threat in aquaculture. *Process Biochem*. 2020;94:213–23.
- Ra G, Do B, Fimia-Duarte R, Mpz G, Contreras Vidal J, Ji, Fez G. International journal of zoology and animal biology committed to create value for researchers. *J Biol Sci*. 2021;4:000301.
- Jensen Ellen C, Schrader Holly S, Rieland B, Thompson Thomas L, Lee Kit W, Nickerson Kenneth W, Kokjohn Tyler A. Prevalence of broad-host-range lytic bacteriophages of *Sphaerotilus natans*, *Escherichia coli*, and *Pseudomonas aeruginosa*. *Appl Environ Microbiol*. 1998;64:575–80.
- Stalin N, Srinivasan P. Efficacy of potential phage cocktails against *Vibrio harveyi* and closely related *Vibrio* species isolated from shrimp aquaculture environment in the South East Coast of India. *Vet Microbiol*. 2017;207:83–96.
- Labrie SJ, Samson JE, Moineau S. Bacteriophage resistance mechanisms. *Nat Rev Microbiol*. 2010;8:317–27.
- Morelli MJ, ten Wolde PR, Allen RJ. DNA looping provides stability and robustness to the bacteriophage  $\lambda$  switch. *Proc Natl Acad Sci*. 2009;106:8101–6.
- Khemayan K, Pasharawipat T, Puiprom O, Sriurairatana S, Suthienkul O, Flegel Timothy W. Unstable lysogeny and pseudolysogeny in *Vibrio harveyi* Siphovirus-Like phage 1. *Appl Environ Microbiol*. 2006;72:1355–63.
- Enderse L, Coffey A. The use of bacteriophages for food safety. *Curr Opin Food Sci*. 2020;36:1–8.
- Chen Y, Li W, Shi K, Fang Z, Yang Y, Zhang R. Isolation and characterization of a novel phage belonging to a new genus against *Vibrio parahaemolyticus*. *Virol J*. 2023;20:81.
- Abdullah AS, Moffat CS, Lopez-Ruiz FJ, Gibberd MR, Hamblin J, Zerihun A. Host–multi-pathogen warfare: pathogen interactions in co-infected plants. 2017, 8.
- Sieben AJ, Mihaljevic JR, Shoemaker LG. Quantifying mechanisms of coexistence in disease ecology. *Ecology*. 2022;103:e3819.
- Kaczmarek J, Jedryczka M. Characterization of two coexisting pathogen populations of *Leptosphaeria* spp., the cause of stem canker of brassicas. *Acta Agrobotanica*. 2011; 64.
- Yu P, Mathieu J, Li M, Dai Z, Alvarez PJJ. Isolation of polyvalent bacteriophages by sequential multiple-host approaches. *Appl Environ Microbiol*. 2016;82:808–15.
- Holtappels D, Alfenas-Zerbini P, Koskella B. Drivers and consequences of bacteriophage host range. *FEMS Microbiol Rev*. 2023;47:fud038.
- Mavrich TN, Hatfull GF. Bacteriophage evolution differs by host, lifestyle and genome. *Nat Microbiol*. 2017;2:17112.
- Piel D, Bruto M, Labreuche Y, Blanquart F, Goudenège D, Barcia-Cruz R, Chenivresse S, Le Panse S, James A, Dubert J, et al. Phage–host Coevolution in natural populations. *Nat Microbiol*. 2022;7:1075–86.

43. Paterson S, Vogwill T, Buckling A, Benmayor R, Spiers AJ, Thomson NR, Quail M, Smith F, Walker D, Libberton B, et al. Antagonistic Coevolution accelerates molecular evolution. *Nature*. 2010;464:275–8.
44. Tu J, Park T, Morado DR, Hughes KT, Molineux IJ, Liu J. Dual host specificity of phage SP6 is facilitated by tailspike rotation. *Virology*. 2017;507:206–15.
45. Meyer JR, Dobias DT, Weitz JS, Barrick JE, Quick RT, Lenski RE. Repeatability and contingency in the evolution of a key innovation in phage lambda. *Science*. 2012;335:428–32.
46. Tétart F, Repoila F, Monod C, Krusch HM. Bacteriophage T4 host range is expanded by duplications of a small domain of the tail fiber adhesin. *J Mol Biol*. 1996;258:726–31.
47. Liu M, Deora R, Doulatov SR, Gingery M, Eiserling FA, Preston A, Maskell DJ, Simons RW, Cotter PA, Parkhill J, Miller JF. Reverse Transcriptase-mediated tropism switching in Bordetella bacteriophage. *Science*. 2002;295:2091–4.
48. Doron S, Fedida A, Hernández-Prieto MA, Sabehi G, Karunker I, Stazic D, Feingersh R, Steglich C, Futschik M, Lindell D, Sorek R. Transcriptome dynamics of a broad host-range cyanophage and its hosts. *ISME J*. 2016;10:1437–55.
49. Howard-Varona C, Roux S, Dore H, Solonenko NE, Holmfeldt K, Markillie LM, Orr G, Sullivan MB. Regulation of infection efficiency in a globally abundant marine bacteriophage virus. *ISME J*. 2017;11:284–95.
50. Howard-Varona C, Hargreaves KR, Solonenko NE, Markillie LM, White RA III, Brewer HM, Ansong C, Orr G, Adkins JN, Sullivan MB. Multiple mechanisms drive phage infection efficiency in nearly identical hosts. *ISME J*. 2018;12:1605–18.
51. Yoshikawa G, Askora A, Blanc-Mathieu R, Kawasaki T, Li Y, Nakano M, Ogata H, Yamada T. Xanthomonas citri Jumbo phage XacN1 exhibits a wide host range and high complement of tRNA genes. *Sci Rep*. 2018; 8.
52. Paul VD, Sundararajan S, Rajagopalan SS, Hariharan S, Kempashanai N, Padmanabhan S, Sriram B, Ramachandran J. Lysis-deficient phages as novel therapeutic agents for controlling bacterial infection. *BMC Microbiol*. 2011;11:195.
53. Costa P, Pereira C, Romalde JL, Almeida A. A game of resistance: war between bacteria and phages and how phage cocktails can be the solution. *Virology*. 2024;599:110209.
54. Blasco L, Blieriot I, González de Aledo M, Fernández-García L, Pacios O, Oliveira H, López M, Ortiz-Cartagena C, Fernández-Cuenca F, Pascual Á, et al. Development of an anti-Acinetobacter baumannii biofilm phage cocktail: genomic adaptation to the host. *Antimicrob Agents Chemother*. 2022;66:e01923–01921.
55. Malone LM, Warring SL, Jackson SA, Warnecke C, Gardner PP, Gumy LF, Fineran PC. A Jumbo phage that forms a nucleus-like structure evades CRISPR-Cas DNA targeting but is vulnerable to type III RNA-based immunity. *Nat Microbiol*. 2020;5:48–55.
56. Leskinen K, Blasdel BG, Lavigne R, Skurnik M. RNA-sequencing reveals the progression of phage-host interactions between  $\phi$ R1-37 and Yersinia enterocolitica. *Viruses*. 2016;8:111.
57. Kiljunen S, Hakala K, Pinta E, Huttunen S, Pluta P, Gador A, Lönnberg H, Skurnik M. Yersiniophage  $\phi$ R1-37 is a tailed bacteriophage having a 270 kb DNA genome with thymidine replaced by Deoxyuridine. *Microbiology*. 2005;151:4093–102.
58. Ceyssens P-J, Minakhin L, Van den Bossche A, Yakunina M, Klimuk E, Blasdel B, De Smet J, Noben J-P, Bläsi U, Severinov K, Lavigne R. Development of giant bacteriophage  $\phi$ KZ is independent of the host transcription apparatus. *J Virol*. 2014;88:10501–10.
59. Illigmann A, Thoma Y, Pan S, Reinhardt L, Brötz-Oesterhelt H. Contribution of the Clp protease to bacterial survival and mitochondrial homeostasis. *Microb Physiol*. 2021;31:260–79.
60. Fernandes AP, Holmgren A. Glutaredoxins glutathione-dependent redox enzymes with functions far beyond a simple thioredoxin backup system. *Antioxid Redox Signal*. 2004;6:63–74.
61. Kim H, Wu K, Lee C. Stress-responsive periplasmic chaperones in bacteria. *Front Mol Biosci*. 2021;8:678697.
62. Darwin AJ. Stress relief during host infection: the phage shock protein response supports bacterial virulence in various ways. *PLoS Pathog*. 2013;9:e1003388.
63. Mendoza SD, Niewegłowska ES, Govindarajan S, Leon LM, Berry JD, Tiwari A, Chaikeratisak V, Pogliano J, Agard DA, Bondy-Denomy J. A bacteriophage nucleus-like compartment shields DNA from CRISPR nucleases. *Nature*. 2020;577:244–8.
64. Bernheim A, Sorek R. The pan-immune system of bacteria: antiviral defence as a community resource. *Nat Rev Microbiol*. 2020;18:113–9.
65. Hussain FA, Dubert J, Elsherbini J, Murphy M, Vanlinsberghe D, Arevalo P, Kauffman K, Rodino-Janeiro BK, Gavin H, Gomez A, et al. Rapid evolutionary turnover of mobile genetic elements drives bacterial resistance to phages. *Science*. 2021;374:488–92.
66. Dedrick RM, Jacobs-Sera D, Bustamante CAG, Garlena RA, Mavrich TN, Pope WH, Reyes JCC, Russell DA, Adair T, Alvey R, et al. Prophage-mediated defence against viral attack and viral counter-defence. *Nat Microbiol*. 2017;2:16251.
67. Beloglazova N, Petit P, Flick R, Brown G, Savchenko A, Yakunin AF. Structure and activity of the Cas3 HD nuclease MJ0384, an effector enzyme of the CRISPR interference. *EMBO J*. 2011;30:4616–27.
68. Magnusson LU, Farewell A, Nyström T. PpGpp: a global regulator in Escherichia coli. *Trends Microbiol*. 2005;13:236–42.
69. Patel PH, Maxwell KL. Prophages provide a rich source of antiphage defense systems. *Curr Opin Microbiol*. 2023;73:102321.
70. Bürkle M, Korf IHE, Lippegaus A, Krautwurst S, Rohde C, Weissfuss C, Nouailles G, Tene XM, Gaborieau B, Ghigo J-M et al. Phage-phage competition and biofilms affect interactions between two virulent bacteriophages and Pseudomonas aeruginosa. *ISME J*. 2025; wraf065.
71. Sasirekha R, Sharma O, Sugumar S. Silico analysis of diversity, specificity and molecular evolution of Stenotrophomonas phages. *Environ Microbiol Rep*. 2022;14:422–30.
72. Roach DR, Donovan DM. Antimicrobial bacteriophage-derived proteins and therapeutic applications. *Bacteriophage*. 2015;5:e1062590.
73. Wang F, Xiong Y, Xiao Y, Han J, Deng X, Lin L. MMPphg from the thermophilic Meiothermus bacteriophage MMP17 as a potential antimicrobial agent against both Gram-negative and Gram-positive bacteria. *Virol J*. 2020;17:130.
74. Ceyssens P-J, De Smet J, Wagemans J, Akulenko N, Klimuk E, Hedger S, Voet M, Hendrix H, Paeshuyse J, Landuyt B, et al. The phage-encoded N-Acetyltransferase Rac mediates inactivation of Pseudomonas aeruginosa transcription by cleavage of the RNA polymerase alpha subunit. *Viruses*. 2020;12:E976.
75. Abedon ST. Lysis from without. *Bacteriophage*. 2011;1:46–9.
76. Kim SG, Kwon J, Giri SS, Yun S, Kim HJ, Kim SW, Kang JW, Lee SB, Jung WJ, Park SC. Strategy for mass production of lytic Staphylococcus aureus bacteriophage pSA-3: contribution of multiplicity of infection and response surface methodology. *Microb Cell Fact*. 2021;20:56.
77. Chatain-LY MH. The factors affecting effectiveness of treatment in phages therapy. 2014;5–2014.
78. Bhoobalan-Chitty Y, Duan X, Peng X. High-MOI induces rapid CRISPR spacer acquisition in Sulfolobus from an Acr deficient virus. *MicroPublication Biology*. 2022.
79. Chen L, Yuan S, Liu Q, Mai G, Yang J, Deng D, Zhang B, Liu C, Ma Y. In vitro design and evaluation of phage cocktails against Aeromonas salmonicida. *Front Microbiol*. 2018;9:2018.
80. Tang Y-j, Yuan L, Chen C-w, Tang A-q, Zhou W-y, Yang Z-q. Isolation and characterization of the new isolated bacteriophage YZU-L1 against Citrobacter freundii from a package-swelling of meat product. *Microb Pathog*. 2023;179:106098.
81. Zhang Y, Jiao N, Roseophage, RDJL $\Phi$ 1. Infecting the aerobic anoxygenic phototrophic bacterium Roseobacter denitrificans OCh114. *Appl Environ Microbiol*. 2009;75:1745–9.
82. Huang C, Zhang Y, Jiao N. Phage resistance of a marine bacterium, Roseobacter denitrificans OCh114, as revealed by comparative proteomics. *Curr Microbiol*. 2010;61:141–7.
83. Kronheim S, Solomon E, Ho L, Glossop M, Davidson AR, Maxwell KL. Complete genomes and comparative analyses of Streptomyces phages that influence secondary metabolism and sporulation. *Sci Rep*. 2023;13:9820.
84. Nair S, Li C, Mou S, Zhang Z, Zhang Y. A novel phage indirectly regulates diatom growth by infecting a diatom-associated biofilm-forming bacterium. *Appl Environ Microbiol*. 2022;88:e02138–02121.
85. Casey E, Mahony J, Neve H, Noben J-P, Dal Bello F, van Sinderen D. Novel phage group infecting Lactobacillus delbrueckii subsp. Lactis, as revealed by genomic and proteomic analysis of bacteriophage Ldl1. *Appl Environ Microbiol*. 2015;81:1319–26.
86. Li C, Wang Z, Zhao J, Wang L, Xie G, Huang J, Zhang Y. A novel vibriophage vB\_VcaS\_HC containing lysogeny-related gene has strong lytic ability against pathogenic bacteria. *Virol Sin*. 2021;36:281–90.
87. Stokar-Avihail A, Fedorenko T, Hör J, Garb J, Levitt A, Millman A, Shulman G, Wojtania N, Melamed S, Amitai G, Sorek R. Discovery of phage determinants that confer sensitivity to bacterial immune systems. *Cell*. 2023;186:1863–e18761816.
88. Pribelski A, Antipov D, Meleshko D, Lapidus A, Korobeynikov A. Using spades de Novo assembler. *Curr Protocols Bioinf*. 2020;70:e102–102.

89. Nayfach S, Camargo AP, Schulz F, Elie-Fadrosh E, Roux S, Kyrpides NC. CheckV assesses the quality and completeness of metagenome-assembled viral genomes. *Nat Biotechnol*. 2021;39:578–85.
90. Besemer J, Lomsadze A, Borodovsky M. GeneMarkS: a self-training method for prediction of gene starts in microbial genomes. Implications for finding sequence motifs in regulatory regions. *Nucleic Acids Res*. 2001;29:2607–18.
91. Seemann T. Prokka: rapid prokaryotic genome annotation. *Bioinformatics*. 2014;30:2068–9.
92. Wang RH, Yang S, Liu Z, Zhang Y, Wang X, Xu Z, Wang J, Li SC. PhageScope: a well-annotated bacteriophage database with automatic analyses and visualizations. *Nucleic Acids Res*. 2023;52:D756–61.
93. Garneau JR, Depardieu F, Fortier L-C, Bikard D, Monot M. PhageTerm: a tool for fast and accurate determination of phage termini and packaging mechanism using next-generation sequencing data. *Sci Rep*. 2017;7:8292.
94. Grant JR, Enns E, Marinier E, Mandal A, Herman EK, Chen C-y, Graham M, Van Domselaar G, Stothard P. Proksee: in-depth characterization and visualization of bacterial genomes. *Nucleic Acids Res*. 2023;51:W484–92.
95. Nishimura Y, Yoshida T, Kuronishi M, Uehara H, Ogata H, Goto S. ViPTree: the viral proteomic tree server. *Bioinformatics*. 2017;33:2379–80.
96. Li C, Shi T, Sun Y, Zhang Y. A novel method to create efficient phage cocktails via use of phage-resistant bacteria. *Appl Environ Microbiol*. 2022;88:e02323–02321.

## Publisher's note

Springer Nature remains neutral with regard to jurisdictional claims in published maps and institutional affiliations.